Available online at www.sciencedirect.com
SCIENCE DIRECT®
Journal of Photochemistry and Photobiology A: Chemistry 162 (2004) 599–607
Journal of Photochemistry and Photobiology A:Chemistry
www.elsevier.com/locate/jphotochem

Photophysical and complexing properties of new fluoroionophores based on coumarin 343 linked to rigidified crown-ethers

D. Taziaux, J.-Ph. Soumillion, J.-L. Habib Jiwan*

Département de Chimie, Unité de Chimie des Matériaux Organiques et Inorganiques (CMAT), Université catholique de Louvain, Place Louis Pasteur 1, B-1348 Louvain-la-Neuve, Belgium

Received 19 June 2003; received in revised form 6 October 2003; accepted 10 October 2003

Abstract

The photophysical and complexing properties of a series of fluoroionophores based on coumarin 343 linked to monoaza-crown ethers are presented. Aiming to modify the selectivity of the fluorescing probe, the complexing cavity is rigidified by the incorporation of benzo groups. Complexation of alkaline-earth cations (magnesium and calcium) induces marked modifications of the photophysical properties of the probes in acetonitrile and in ethanol, whereas the alkaline cations induce only very weak modifications. The stoichiometry of the complexes is 1:1, except for C343-crown and C343-benzocrown in acetonitrile, where two complexes can be formed with calcium. The results obtained show that rigidification of the complexing cavity improves selectivity, favouring the complexation of Mg^{2+} and Ca^{2+} versus Li^{+}. Competition between Mg^{2+} and Ca^{2+} has also been studied.

Keywords: Fluoroionophore; Crown-ether

1. Introduction

The development of chromogenic and fluorogenic molecular sensors for metal cations has been the object of important effort due to a broad variety of potential applications [1–3]. The design principles of the so-called fluoroionophores consisting of a fluorophore linked to a complexing unit have been reviewed [4–6]. In these host–guest systems, the photophysical properties of the fluorophore are modified by the complexation of a cation in the ionophore cavity. This opens the way to the recognition and determination of metal cation concentration. Various photoinduced processes, such as electron, charge or energy transfer, and excimer formation or disappearance, might be responsible for these photophysical modifications.

Coumarins with an electron-donating group in position 7 are interesting fluorophores to be attached to an ionophore. The electron-donating group is conjugated with the carbonyl of the lactone ring, which acts as an electron-withdrawing group. Since this carbonyl may participate to the complexation of a metal cation chelated by a crown-ether linked on that side of the coumarin, marked photophysical changes are expected and have been observed [7].

In a previous paper, we have reported the photophysical and complexing properties of a fluoroionophore composed of a coumarin C343 linked to a 1-aza-15-crown-5 (C343-crown) via an amide bridge [8]. It was demonstrated that the introduction of an amide bridge instead of the widely used methylene bridge has interesting effects. First of all, the selectivity for alkaline-earth cations versus alkaline cations is much better for C343-crown (only Li^{+} is complexed) than for C153-crown (all alkaline cations were complexed [7]). This might be due to the presence of a less flexible bridge.

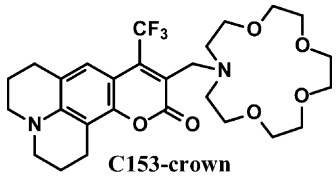

C153-crown

Moreover, additional photophysical effects result from the presence of the amide function: when the ionophore cavity is occupied by a cation, the linking amide behaves as an electron withdrawing group and induces hyperchromicity as well as additional shifts.

In order to try to improve the selectivity, we have replaced the monoaza-15-crown-5 by monoaza-15-benzocrown-5 and monoaza-15-dibenzocrown-5. The benzo groups should

* Corresponding author. Tel.: +32-1047-8909; fax: +32-1047-9178.
E-mail address: habib@chim.ucl.ac.be (J.-L. Habib Jiwan).

1010-6030/$ – see front matter © 2004 Elsevier B.V. All rights reserved.
doi:10.1016/S1010-6030(03)00424-6

rigidify the complexing cavity and modifications of the selectivity may be expected.

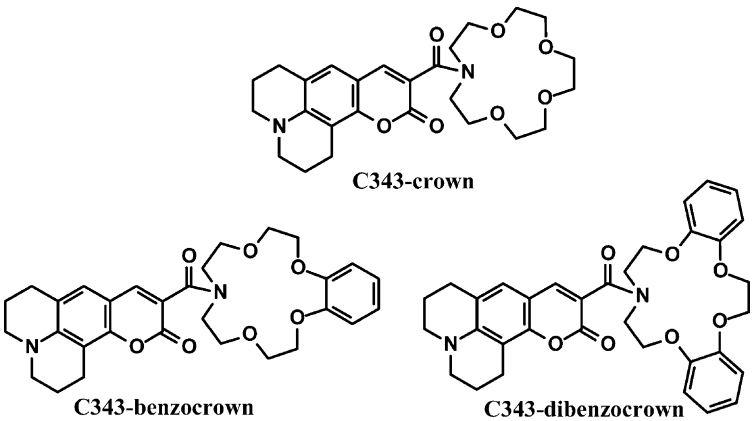

2. Materials and methods

2.1. Solvents and reagents

Acetonitrile from Fluka (HPLC grade) and ethanol from Merck (spectrometric grade) were used as solvents for absorption and fluorescence measurements. Lithium, sodium, alkaline-earth perchlorates and potassium thiocyanate purchased from Alpha were of the highest quality available and vacuum dried on P_2O_5 prior to use. Coumarin 343 and 1-aza-15-crown-5 were purchased from Aldrich, azabenzo15-crown-15 was a Fluka product and they were used without further purification.

2.2. Apparatus

Infrared spectra were obtained on a Biorad spectrophotometer, using KBr pellets. UV-Vis spectra were recorded on a Varian Cary 5E spectrophotometer. Corrected emission spectra were obtained on a SML Aminco 48000 spectrofluorometer. Fluorescence quantum yields were determined using Coumarin 314 as a reference (Φ=0.68 in ethanol [9]).

The fluorescence decay times were measured by single photon counting with a PicoQuant Fluotime 200 set-up. The excitation source is a Coherent Mira 900F pumped by a Verdi 10W delivering pulses of approximately 130 fs. The repetition rate of the Mira is reduced to 3.8 MHz with a Coherent Pulse-Picker 9200 and the frequency is doubled by a Mira 9300 harmonic generator. The overall instrument response function is below 30 ps. The decay traces were deconvoluted with the PicoQuant Fluofit software.

NMR spectra were recorded on a Varian Gemini 300 and mass spectra on a Finnigan Matt TSQ-7000, by electronic impact or fast atom bombardment.

HPLC analyses were performed with a SpectraPhysics SP 8800, equipped with a C18 reverse phase column. Analyses were done at two wavelengths (240 and 380 nm), with an EtOH–water (70:30) eluent.

2.3. Synthesis

Aza dibenzo15-crown-5 was synthesised according to the method of Vaidya et al. [10].

The fluoroionophores were synthesised by reacting Coumarin 343 with the corresponding aza-crown via the acyl chloride according to [8].

2.3.1. C343-crown

See [8] for more details.

2.3.2. C343-benzocrown

The crude product was purified first by flash chromatography on silica (eluent: CH_2Cl_2–iPrOH (98:2)), then recrystallised from AcOEt and pentane, to give 171 mg (40%) of yellow powder, melting point: 157 °C.

Purity: 99.6% (HPLC).

^{1}H NMR ($CDCl_3$) δ (ppm): 1.95 (m, 4H); 2.73 (t, 2H); 2.86 (t, 2H); 3.29 (2t, 4H); 3.59 (m, 2H); 3.75–3.80 (m, 4H); 3.89 (m, 6H); 4.19 (m, 4H); 6.79 (s, 1H); 6.91 (m, 4H); 7.59 (s, 1H).

MS (FAB-MNBA) (*m*/*z*): 535 (MH$^+$), 268.

FTIR (KBr pellet): wave number (cm^{-1}): 2922, 2857, 1707, 1620, 1598, 1562, 1508, 1445, 1370.

$C_{30}H_{34}N_2O_7$ requires C: 67.40, H: 6.41, N: 5.24, found: C: 66.13, H: 6.08, N: 4.92.

2.3.3. C343-dibenzocrown

The crude product is purified by flash chromatography on silica, eluent: CH_2Cl_2–iPrOH (98:2), followed by crystallisation from EtOH and pentane, to give 200 mg (38%) of yellow powder, melting point: 155 °C.

Purity: 99.5% (HPLC).

^{1}H NMR ($CDCl_3$) δ (ppm): 1.95 (m, 4H); 2.73 (t, 2H); 2.88 (t, 2H); 3.29 (m, 2H); 3.82 (m, 2H); 4.02 (m, 2H); 4.39 (m, 8H); 6.81 (s, 1H); 6.93 (m, 8H); 7.91 (s, 1H).

MS (FAB-NMBA) (*m*/*z*): 583.1 (MH$^+$), 276.9.

FTIR (KBr pellet) wave number (cm^{-1}): 2932, 2851, 1715, 1616, 1601, 1561, 1502, 1445, 1370.

$C_{34}H_{34}N_2O_7$ requires C: 70.13, H: 5.84, N: 4.81, found: C: 70.33, H: 5.86, N: 4.63.

2.4. Stability constants determination

In the case of stoichiometry 1:1, the equilibrium is controlled by a stability constant expressed by K_1 (Eq. (1)) where [L], [M] and [ML] are the concentrations of the free ligand, free metal ion and complex, respectively. The commonly used Eq. (2) can easily be derived.

$$\mathrm{ML} \leftrightarrows \mathrm{M} + \mathrm{L} \qquad K_1 = \frac{[\mathrm{ML}]}{[\mathrm{M}][\mathrm{L}]} \tag{1}$$

$$\frac{X_0 - X}{X - X_{\mathrm{lim}}} = K_{\mathrm{S}}[\mathrm{M}] \tag{2}$$

where X is the absorbance or the fluorescence of the solution, X_0 and X_{lim} are the values of X for the free ligand and for the ML complex, respectively.

It is often assumed that C_{M}, the total concentration of metal ion, is equal to [M]. However, when the efficiency of complexation is very high, this approximation cannot be done and it is then necessary to derive Eq. (3), where C_0 is the total ligand concentration [8]

$$X = X_0 + \frac{X_{\mathrm{lim}} - X_0}{2C_0}\left[C_0 + C_{\mathrm{M}} + \frac{1}{K_{\mathrm{S}}} - \left[\left(C_0 + C_{\mathrm{M}} + \frac{1}{K_{\mathrm{S}}}\right)^2 - 4C_0C_{\mathrm{M}}\right]^{1/2}\right] \tag{3}$$

K_{S} can then be obtained by a non-linear least square analysis of X versus C_{M}. If X_{lim} cannot be accurately determined, it can be left as a floating parameter in the analysis.

For the 2:1 stoichiometry, successive complexations according to the following scheme were considered and the Eq. (4) was derived [8].

$$\mathrm{M} + \mathrm{L} \leftrightarrows \mathrm{ML} \qquad K_1 = \frac{[\mathrm{ML}]}{[\mathrm{M}][\mathrm{L}]}$$

$$\mathrm{ML} + \mathrm{L} \leftrightarrows \mathrm{M_2L} \qquad K_2 = \frac{[\mathrm{M_2L}]}{[\mathrm{ML}][\mathrm{M}]}$$

$$X = \frac{X_0 + C_0bK_1[\mathrm{M}] + X_{\mathrm{lim}}\beta[\mathrm{M}]^2}{1 + K_1[\mathrm{M}] + \beta[\mathrm{M}]^2} \tag{4}$$

where $\beta = K_1K_2$ and b is the absorptivity of the intermediate complex ML. This expression can be used under the approximation $[\mathrm{M}] \cong C_{\mathrm{M}}$. K_1 and b can be determined by a non-linear least square analysis of X versus C_{M}.

For the 3:2 stoichiometry, the following successive complexations were considered, leading to Eq. (5) [8].

$$\mathrm{M} + \mathrm{L} \leftrightarrows \mathrm{ML} \qquad K_1 = \frac{[\mathrm{ML}]}{[\mathrm{M}][\mathrm{L}]}$$

$$2\mathrm{ML} + \mathrm{M} \leftrightarrows \mathrm{M_3L_2} \qquad K_2 = \frac{[\mathrm{M_3L_2}]}{[\mathrm{ML}]^2[\mathrm{M}]}$$

$$X = \frac{N}{4K_1^2K_2[\mathrm{M}]^3C_0}\left(X_0 + bC_0K_1[\mathrm{M}] + \frac{X_{\mathrm{lim}}N}{2}\right) \tag{5}$$

in which

$$N = -1 - K_1[\mathrm{M}] + \{(1 + K_1[\mathrm{M}])^2 + 8C_0K_1^2K_2[\mathrm{M}]^3\}^{1/2}$$

3. Results and discussion

The fluoroionophores were synthesised by coupling the acyl chloride of coumarin C343 to the azacrown ether. Monoaza-15-dibenzocrown-5 was prepared according to the method reported by Vaidya et al. [10]. Most of the experiments with C343-crown were reproduced in order to have the best comparison possible with the new fluoroionophores.

3.1. Cation-induced photophysical changes in acetonitrile

Results are reported in Tables 1 and 2 and the spectrum evolution of C343-dibenzocrown upon addition of magnesium perchlorate is illustrated in Fig. 1.

Table 1
Absorption properties in acetonitrile at room temperature

	Radius[a] (Å)	Charge density[b] ($q \times Å^{-1}$)	C343-crown			C343-benzocrown			C343-dibenzocrown		
			λ_{max} (nm)	$\varepsilon \times 10^{-3}$ ($M^{-1}\,cm^{-1}$)	λ_{iso} (nm)	λ_{max} (nm)	$\varepsilon \times 10^{-3}$ ($M^{-1}\,cm^{-1}$)	λ_{iso} (nm)	λ_{max} (nm)	$\varepsilon \times 10^{-3}$ ($M^{-1}\,cm^{-1}$)	λ_{iso} (nm)
Ligand	0.85–1.10	–	410.0	27.4	–	410.5	28.7	–	412.3	28.0	–
Li^+	0.90	1.11	424.0	28.7	415.0	419.3	27.9	415.0	418.3	28.3	414.3
Na^+	1.16	0.86	414.0	–[c]	412.0	411.5	28.8	–[c]	413.5	28.6	–[c]
K^+	1.52	0.66	410.0	–[c]	–[c]	413.3	28.1	412.5	413.0	28.5	–[c]
Mg^{2+}	0.86	2.32	452.0	38.8	423.5	456.5	39.8	426.0	458.0	36.4	427.0
Ca	1.14	1.75	450.0	41	422.0	446.8	33.5	421.5	445.5	36.0	423.0

λ_{max}: absorption maximum; ε: molar absorption coefficient; λ_{iso}: wavelength of the isosbestic point.

[a] For the ligand: radius of the cavity of crown-ether 15-crown-5 [13]; for the cations: radius for a co-ordination number of 6 (Shannon table) [14].

[b] Number of charge/radius.

[c] The cation-induced changes are too small to yield a reliable value characteristic of the complex.

Table 2
Emission properties in acetonitrile at room temperature

	Radius[a] (Å)	Charge density[b] ($q \times Å^{-1}$)	C343-crown				C343-benzocrown				C343-dibenzocrown			
			λ_{em} (nm)	Φ_F	τ (ns)	Amplitude (%)	λ_{em} (nm)	Φ_F	τ (ns)	Amplitude (%)	λ_{em} (nm)	Φ_F	τ (ns)	Amplitude (%)
Ligand	0.85–1.10	–	473	0.65	3.63		475	0.65	3.66		475	0.64	3.65	
Li^+	0.90	1.11	487	[c]	4.05		490	0.63	3.77		492	0.56	3.70	
Na^+	1.16	0.86	[c]	[c]	[c]		[c]	[c]	[c]		[c]	[c]	[c]	
K^+	1.52	0.66	[c]	[c]	[c]		[c]	[c]	[c]		[c]	[c]	[c]	
Mg^{2+}	0.86	2.32	498	0.66	4.28	92.5	502	0.62	4.28	91.4	504	0.70	4.29	90.4
					1.71	7.5			1.15	8.6			1.61	9.6
Ca^{2+}	1.14	1.75	496	0.65	4.09		499	0.63	4.07		499	0.69	4.71	92.2
													1.48	7.8

λ_{em}: emission maximum; Φ_F: fluorescence quantum yield, estimated error maximum 10%; τ: fluorescence decay times, satisfactory values of the reduced χ^2 were found in all cases.
[a] For the ligand: radius of the cavity of crown-ether 15-crown-5 [13]; for the cations: radius for a co-ordination number of 6 (Shannon table) [14].
[b] Number of charge/radius.
[c] The cation-induced changes are too small to yield a reliable value characteristic of the complex.

The replacement of the aza-crown by aza-benzocrown has a negligible effect on the spectral properties, a red shift of maximum 2 nm is observed.

The effects of calcium and magnesium cations on C343-benzocrown and C343-dibenzocrown are similar to those reported for C343-crown [8]. The absorption spectrum undergoes an important red shift from 410 to 456 nm for C343-dibenzocrown at full complexation with Mg^{2+}, whereas a smaller shift of the emission spectrum (29 nm) is recorded. Addition of alkali metal ions induces much weaker effects (Fig. 2); Na^+ and K^+ even at high concentration give almost negligible changes, whereas Li^+ induces significant shifts in absorption and emission.

These spectral shifts may be understood in terms of cation–dipole interaction because the chelated cation can interact with the carbonyl groups (lactone, amide or both) of the coumarinic fluorophore (Scheme 1). The dipole moment of the coumarin is higher in the excited state than in the ground state as a result of the photoinduced charge transfer from the nitrogen atom of the julolidyl ring to the conjugated carbonyl groups [11]. Therefore, in the presence of a cation bound to these groups, the excited state is stabilised to a greater extent than the ground state so that the absorption and emission spectra are red shifted [12].

An increase of the molar absorption coefficient due to the metal complexation has been observed in the case of C343-crown [8] and is still present for the new fluoroionophores. This was explained by an electron withdrawing effect of the metal cation bound amide carbonyl on the coumarin. The presence of this effect for C343-benzocrown and C343-dibenzocrown reveals the participation of the amide carbonyl to the metal chelation.

It should be noted that the absorption spectral shift induced by Li^+ decreases with the introduction of benzo groups in the ionophoric cavity: 14 nm for C343-crown, 9 nm for C343-benzocrown and 6 nm for C343-dibenzocrown. This might be due to the rigidification of the ionophoric cavity which precludes a shrinkage of the cavity around the small lithium cation, therefore, a weaker stabilising interaction is expected between the cation and the carbonyl groups. On the other hand, the emission spectral shift due to the Li^+ chelation is not reduced by the introduction of the benzo group, a slight increase is even observed (from 14 nm for C343-crown to 17 nm for C343-dibenzocrown). A possible explanation is a movement of the lithium cation closer to the carbonyls during the lifetime of the excited state. This motion would be driven by a strong electrostatic

Scheme 1. Proposed structure for an ML complex.

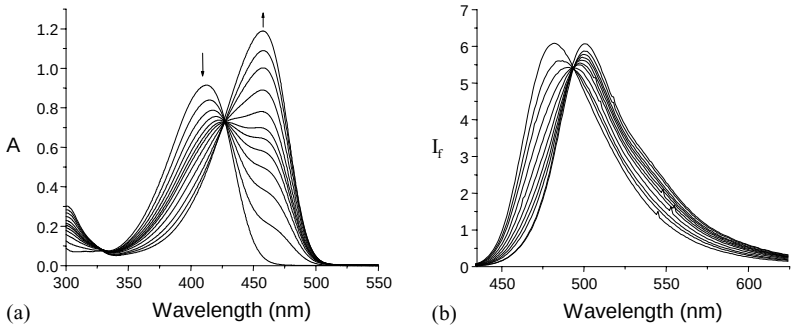

Fig. 1. Evolution of the absorption (a) and fluorescence (b) spectrum of C343-dibenzocrown upon addition of magnesium perchlorate.

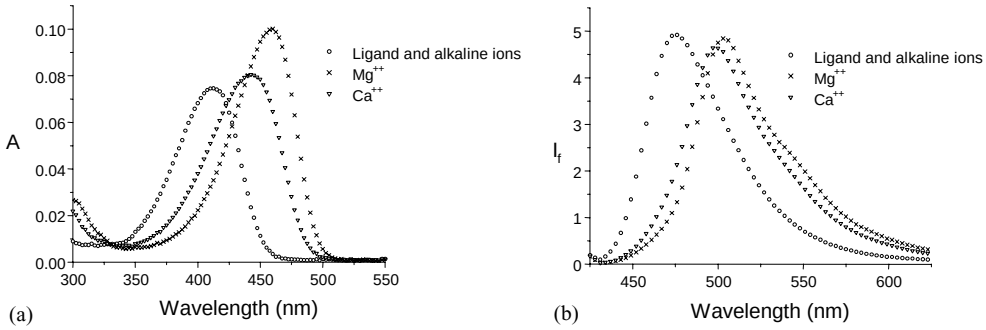

Fig. 2. Absorption (a) and emission (b) spectra of free C343-dibenzocrown and at full complexation with cations.

attraction between Li^+ and the important negative charge density of the lactone moiety of the coumarin in the excited state.

The incorporation of benzo groups to the complexing cavity has almost no influence on the photophysical properties of the free ligands. However, an increase of the gap between the absorption maxima of the Ca^{2+} and Mg^{2+} complexes is induced (this gap is of 3, 10 and 13 nm, for C343-crown, C343-benzocrown, C343-dibenzocrown, respectively). This effect deserves to be underlined since it allows an easier discrimination between Mg^{2+} and Ca^{2+} and thus, might be viewed as a photophysical selectivity.

The fluorescence quantum yield and the fluorescence decay time of the fluoroionophores are only slightly affected by the metal chelation (see Table 2). Nevertheless, it is worthwhile to note that biexponential decays are observed, in the case of magnesium complexes with the three fluoroionophores. In the calcium case, a biexponential decay is observed only for the C343-dibenzocrown complex. The observation of biexponential decays might be an indication for a mixture of different complexes or at least of different excited states. The shoulder (stronger for Mg^{2+} than for Ca^{2+}) displayed on the emission spectra of the complexes (Fig. 2), gives further hints for this explanation.

By calculating the radiative and non-radiative rate constants from the values of the fluorescence quantum and the excited state lifetime, it appears that the non-radiative rate constant is significantly decreased by the chelation with magnesium or calcium cation. This might be due to a rigidification of the fluoroionophore upon complexation, namely an inhibition of the rotation around the amide bridge.

3.2. Cation-induced photophysical changes in ethanol

In ethanol, the general trends of the changes in photophysical properties on cation binding resemble those in acetonitrile. Results are presented in Tables 3 and 4. Once more, the effects of cation addition are stronger for calcium and magnesium than for lithium, sodium and potassium. For these cations, there is almost no change in the absorption and emission spectra of the ligand even on addition of large amounts of cation. It is worth to note that, in ethanol, magnesium and calcium induce a biexponential decay for all the three fluoroionophores.

3.3. Stoichiometry and stability constants of the complexes

The stability constants were obtained using the evolution of the absorption spectra of ligand solution ([ligand] $\cong 3 \times 10^{-5}$ M) upon addition of metal ions. The experimental data were processed by Origin© software. In most cases, the titration curves can be satisfactorily fitted to an ML stoichiometry.

The results for lithium, magnesium and calcium complexes are reported in Table 5 and an example of titration curve is given in Fig. 3 for C343-dibenzocrown with magnesium and calcium.

Table 3
Absorption properties in ethanol at room temperature

	Radius[a] (Å)	Charge density[b] ($q \times Å^{-1}$)	C343-crown			C343-benzocrown			C343-dibenzocrown		
			λ_{max} (nm)	$\varepsilon \times 10^{-3}$ ($M^{-1}\,cm^{-1}$)	λ_{iso} (nm)	λ_{max} (nm)	$\varepsilon \times 10^{-3}$ ($M^{-1}\,cm^{-1}$)	λ_{iso} (nm)	λ_{max} (nm)	$\varepsilon \times 10^{-3}$ ($M^{-1}\,cm^{-1}$)	λ_{iso} (nm)
Ligand	0.85–1.10	–	415.5	29.0	–	416.0	29.3	–	418.5	27.7	–
Li^+	0.90	1.11	417.0	–[c]	415.5	417.0	29.8	–[c]	419.0	28.0	–[c]
Na^+	1.16	0.86	419.0	–[c]	412.0	417.0	29.9	–[c]	419.0	27.9	–[c]
K^+	1.52	0.66	418.0	–[c]	–[c]	417.0	30.2	–[c]	419.0	27.9	–[c]
Mg^{2+}	0.86	2.32	452.0	40.1	423.5	452.5	39.9	426.0	454.0	38.5	428.5
Ca	1.14	1.75	436.0	33.0	422.0	433.0	31.3	420.0	435.0	29.5	424.0

λ_{max}: absorption maximum; ε: molar absorption coefficient; λ_{iso}: wavelength of the isosbestic point.
[a] For the ligand: radius of the cavity of crown-ether 15-crown-5 [13]; for the cations: radius for a co-ordination number of 6 (Shannon table) [14].
[b] Number of charge/radius.
[c] The cation-induced changes are too small to yield a reliable value characteristic of the complex.

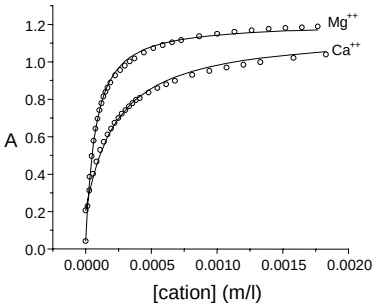

Fig. 3. Titration curves of C343-dibenzocrown with magnesium and calcium perchlorates. The solid lines represent the fits with Eq. (3).

For the Na^+ and K^+, the photophysical changes were too small for a reliable determination of the stability constants, which are probably very small.

In acetonitrile, the most striking effect of the rigidification of the complexing cavity is observed for lithium. The values of the stability constants of the complexes formed by C343-crown with Li^+, Mg^{2+}, Ca^{2+} are rather close. The introduction of a first benzo group allowed to reach a better selectivity of detection of the alkaline-earth cations versus Li^+ with a complexation of lithium which is less efficient by two orders of magnitude. For C343-dibenzocrown, the complexation of lithium is still weakened and no reliable value of K_S could be obtained.

All those values can be explained in terms of size and charge density of the cations. Ca^{2+} is, probably, the cation whose diameter fits the best in the crowned complexing cavity. Li^+ and Mg^{2+} are smaller than the hosting cavity, but in the case of C343-crown, the flexibility of the cavity probably allows it to tighten around those small cations. Introducing benzo groups should induce a rigidification of the complexing aza-crown cavity and thereby reduce the tightening capacity around small cations. This can explain the drop of the stability constant for lithium, for C343-benzocrown and the absence of measurable complexation for C343-dibenzocrown.

The lack of selectivity between magnesium (of which the ionic diameter is close to lithium) and calcium can be explained by the difference of charge density. With its high charge density, Mg^{2+} must be able to interact at a larger distance with the receptor, and specifically with the carbonyl and the amide links. On the other hand, the stability constants for Mg^{2+} with the three fluoroionophores are very close in acetonitrile ($\log K_S = 4.27$, 4.59 and 4.24 for C343-crown, C343-benzocrown and C343-dibenzocrown, respectively). This absence of effect of the modification of the crown-ether may indicate that the complexing crown does not really participate to the Mg^{2+} chelation. Magnesium cation could be preferentially chelated by the two carbonyl groups of the fluoroionophore (Scheme 2). Such kind of supramolecular structure was recently proposed by Alonso et al. [15] for other coumarin-derived ionophores.

As in the previously reported case of C343-crown [8], the complex formed by C343-benzocrown with Ca^{2+} in

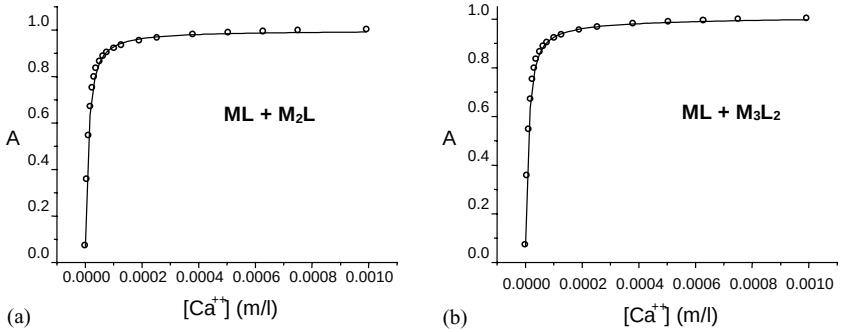

Fig. 4. Titration curve of C343-crown with calcium perchlorate. The solid line represents the best fit with Eq. (4) (a) and with Eq. (5) (b).

Table 4
Emission properties in ethanol at room temperature

	Radius[a] (Å)	Charge density[b] ($q \times Å^{-1}$)	C343-crown				C343-benzocrown				C343-dibenzocrown			
			λ_{em} (nm)	Φ_F	τ (ns)	Amplitude (%)	λ_{em} (nm)	Φ_F	τ (ns)	Amplitude (%)	λ_{em} (nm)	Φ_F	τ (ns)	Amplitude (%)
Ligand	0.85–1.10	–	479	0.67	3.89		481	0.67	3.94		481	0.69	3.61	
Li^+	0.90	1.11	_[c]	_[c]	_[c]		_[c]	_[c]	_[c]		_[c]	_[c]	_[c]	
Na^+	1.16	0.86	_[c]	_[c]	_[c]		_[c]	_[c]	_[c]		_[c]	_[c]	_[c]	
K^+	1.52	0.66	_[c]	_[c]	_[c]		_[c]	_[c]	_[c]		_[c]	_[c]	_[c]	
Mg^{2+}	0.86	2.32	495	0.66	4.10	89.2	497	0.67	4.16	89.7	500	0.69	4.13	86.3
					1.03	10.8			0.99	10.3			0.94	13.7
Ca^{2+}	1.14	1.75	491	0.64	4.00	81.5	494	0.68	4.03	82.4	496	0.69	3.99	80.7
					0.85	18.5			0.95	17.6			0.87	19.3

λ_{em}: emission maximum; Φ_F: fluorescence quantum yield, estimated error maximum 10%; τ: fluorescence decay times, satisfactory values of the reduced χ^2 were found in all cases.
[a] For the ligand: radius of the cavity of crown-ether 15-crown-5 [13]; for the cations: radius for a co-ordination number of 6 (Shannon table) [14].
[b] Number of charge/radius.
[c] The cation-induced changes are too small to yield a reliable value characteristic of the complex.

Table 5
Stability constants

Solvent	Cation	C343-crown ($\log K_g$)	C343-benzocrown ($\log K_g$)	C343-dibenzocrown ($\log K_g$)
Acetonitrile	Li^+	3.26 ± 0.01	1.77 ± 0.02	–[a]
	Mg^{2+}	4.72 ± 0.02	4.59 ± 0.0l	4.24 ± 0.01
	Ca^{2+}	–[b]	–[b]	3.65 ± 0.01
Ethanol	Mg^{2+}	3.08 ± 0.02	2.29 ± 0.01	2.73 ± 0.02
	Ca^{2+}	2.78 ± 0.01	2.78 ± 0.01	2.06 ± 0.02

[a] The modifications induced by complexation are very low, no reliable value of K_S could be obtained.
[b] Unsatisfactory fit with ML model. Other stoichiometries are considered below.

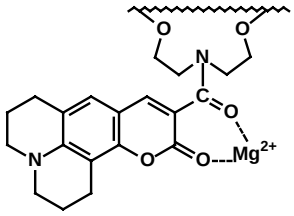

Scheme 2. Possible structure for the Mg^{2+} complexes in acetonitrile.

acetonitrile does not give a satisfactory fit with ML stoichiometry. ML_2 and M_3L_2 complexes were then considered. The stability constants obtained are reported in Table 6. Both stoichiometries fitted satisfactorily with the experimental datas (see Fig. 4) and it was not possible to discriminate between them.

3.4. Competition experiments

Mg^{2+} and Ca^{2+} both play an important biological role. Their selective detection is thus of high interest. Many fluorescent sensors have been developed for the measurement of Ca^{2+} concentration in biological samples [16]. Fewer have been developed for Mg^{2+} [17] and most of the fluoroionophores reported are only useful for Mg^{2+} concentration much higher than Ca^{2+}, when their respective extracellular concentrations, both in the micromolar range, are quite close.

Competitive experiments have been performed with C343-dibenzocrown in order to check if the selective detection of Mg^{2+} in presence of Ca^{2+} was possible. The selectivity (expressed as the ratio of the stability constants) Mg^{2+}/Ca^{2+} is only 3.89, yet discrimination might be possible thanks to the gap between the absorption maxima of the Mg^{2+} and Ca^{2+} complexes.

Table 6
Stability constants for Ca^{2+}

	C343-crown ($\log K_g$)	C343-benzocrown ($\log K_g$)
ML	(5.58)[a]	(4.68)[a]
M_2L	3.97 ± 0.77	5.46 ± 0.13
	5.32 ± 0.09	9.33 ± 0.19
M_3L	4.11 ± 0.07	5.15 ± 0.13
	10.30 ± 0.10	18.50 ± 0.37

[a] Unsatisfactory fit.

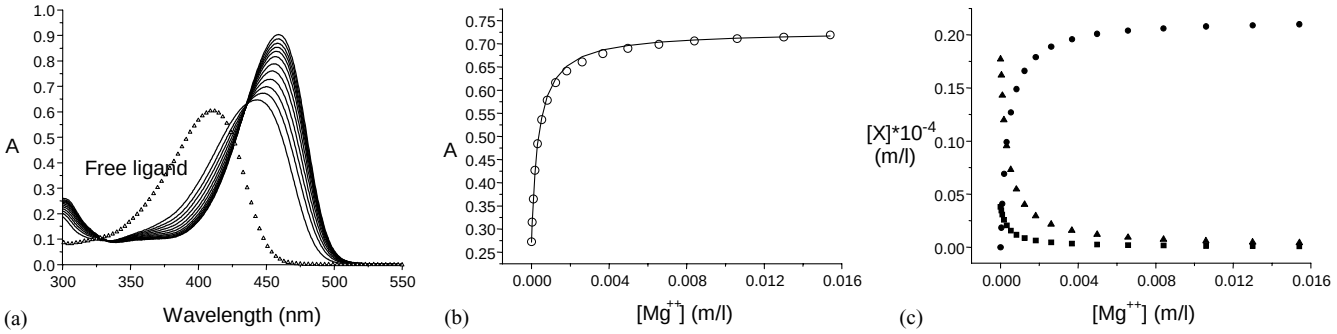

Fig. 5. Evolution of the absorption spectrum of C343-dibenzocrown + 1 mM $Ca(ClO_4)_2$ (a), titration curve (b) and evolution of the different species' concentration ((■) free ligand, (●) MgL, (▲) CaL) (c) upon addition of $Mg(ClO_4)_2$ in acetonitrile.

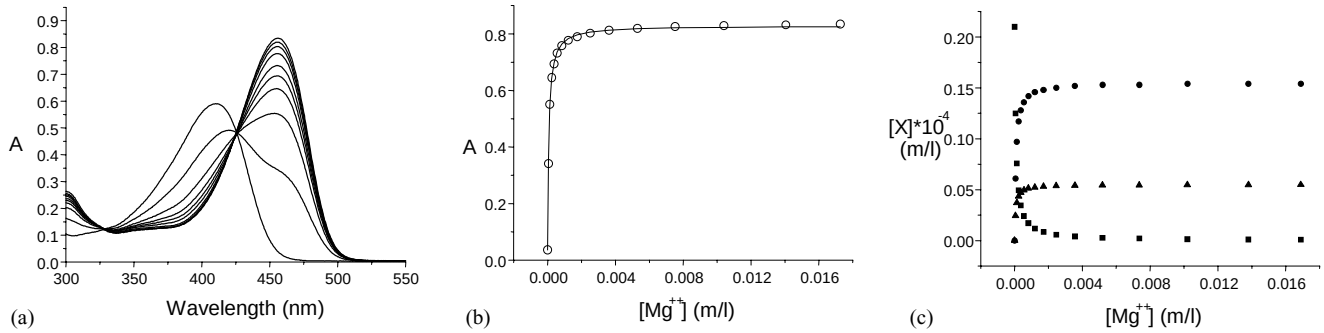

Fig. 6. Evolution of the absorption spectrum of C343-dibenzocrown (a), titration curve (b) and evolution of the different species' concentration ((■) free ligand, (●) MgL, (▲) CaL) (c) upon addition of $Mg(ClO_4)_2$–$Ca(ClO_4)_2$ (1:1) in acetonitrile.

In a first experiment, C343-dibenzocrown was titrated with Mg^{2+} in presence of 1 mM Ca^{2+}, in acetonitrile. The evolution of the absorption spectrum and the titration curve, illustrated in Fig. 5, clearly show that Mg^{2+} can be detected when Ca^{2+} is present, with a very good sensitivity.

Those results were processed by Specfit© software, using the known spectra of the free ligand, MgL and CaL complexes. In presence of 1 mM Ca^{2+}, $\log K_S$ for Mg^{2+} is 4.20± 0.01, which is very close to the value obtained for Mg^{2+} alone. The magnesium complex being more stable than the calcium complex, the latter disappears as $Mg(ClO_4)_2$ is added.

A second experiment was performed in which the probe was titrated with a solution containing both cations at the same concentration. These results are illustrated by Fig. 6. Processing with Specfit© gave $\log K_S = 3.57 \pm 0.02$ for Ca^{2+}, and $\log K_S = 4.02 \pm 0.01$ for Mg^{2+}. These values are in good agreement with those obtained for the separate cations (see Table 5).

4. Conclusion

The rigidification of the complexing cavity by incorporation of benzo groups greatly improved the selectivity of detection of the alkaline-earth cations versus Li^+. Indeed, if the stability constant obtained for the lithium complex of C343-crown was close to those obtained for the alkaline-earth complexes, it's much lower for C343-benzocrown. For C343-dibenzocrown, the interaction with Li^+ was so weak that no constant could be determined.

The addition of benzo groups to the complexing cavity also increased the gap between the absorption maxima of the magnesium and calcium complexes, allowing an easier deconvolution of the spectra when those cations are both present.

Acknowledgements

The authors gratefully acknowledge the "Fonds National de la Recherche Scientifique" for its financial support through the "FRFC No. 2.4531.99, the Université catholique de Louvain through the "FSR and COSIF 1998". D.T. thanks the FRIA for a predoctoral fellowship. Discussions with Dr. I. Leray (ENS-Cachan) and Professor B. Valeur (CNAM and ENS-Cachan) were highly appreciated.

References

[1] A.W. Czarnik (Ed.), Fluorescent chemosensors for ion and molecule recognition, ACS Symposium Series 538, American Chemical Society, Washington, DC, 1992.
[2] J.R. Lakowicz (Ed.), Topics in Fluorescence Spectroscopy, Probe Design and Chemical Sensing, vol. 4, Plenum, New York, 1992.

[3] J.P. Desvergne, A.W. Czarnik (Ed.), Chemosensors for ion and molecule recognition, NATO ASI Series, Kluwer Academic Publishers, Dordrecht, 1997.
[4] B. Valeur, I. Leray, Coord. Chem. Rev. 205 (2000) 3.
[5] B. Valeur, Molecular Fluorescence—Principles and Applications, Fluorescent Molecular Sensors of Ions and Molecules, Wiley-VCH, Weinheim, 2002 (Chapter 10).
[6] A.P. de Silva, H.Q.N. Gunaratne, T. Gunnlaugsson, A.J.M. Huxley, C.P. McCoy, J.T. Rademacher, T.E. Rice, Chem. Rev. 97 (1997) 1515.
[7] J. Bourson, J. Pouget, B. Valeur, J. Phys. Chem. 97 (1993) 4552.
[8] J.-L. Habib Jiwan, C. Branger, J.-P. Soumillion, B. Valeur, J. Photochem. Photobiol. A: Chem. 116 (1998) 127.
[9] G.A. Reynolds, K.H. Drexhage, Optic. Commun. 13 (1975) 222.
[10] B. Vaidya, J. Zak, G.J. Bastiaans, M.D. Porter, Anal. Chem. 67 (1995) 4101.
[11] A. Samanta, R.W. Fessenden, J. Phys. Chem. A 104 (2000) 8577.
[12] B. Valeur, Principles of fluorescent probe design for ion recognition in ref. [2].
[13] C.J. Perdersen, K. Frensdorff, Angew. Chem. 11 (1972) 16.
[14] R.D. Shannon, Acta Crystallogr. A 32 (1976) 751.
[15] M.-T. Alonso, E. Brunet, O. Juanes, J.-C. Rodriguez-Ubis, J. Photochem. Photobiol. A: Chem. 174 (2002) 113.
[16] D.C. Lambert (Ed.), Calcium Signaling Protocols (Methods in Molecular Biology), Humana Press, Clifton, UK, 1999.
[17] R.E. London, Annu. Rev. Physiol. 53 (1991) 241–258.